First-principles calculation of elastic properties of solid argon at high pressures

Toshiaki Iitaka[#] and Toshikazu Ebisuzaki

Computational Science Division, Advanced Computing Center, RIKEN

The density and the elastic stiffness coefficients of fcc solid argon at high pressures from 1 GPa up to 80 GPa are computed by the first-principles pseudopotential method with the plane-wave basis set and the generalized gradient approximation (GGA). The result is in good agreement with the experimental result recently obtained by means of Brillouin spectroscopy by Shimizu *et al*. [Phys. Rev. Lett. **86**, 4568 (2001)]. The Cauchy condition was found to be strongly violated as in the experimental result, indicating a large contribution from the non-central many-body force. The present result has clarified that the standard density functional method with periodic boundary conditions can be applied for calculating the elastic properties of rare gas solids at high pressures in contrast to those at low pressures where dispersion forces are important.

Introduction

Rare gas atoms are among the simplest substances in terms of physical and chemical properties because of their closed-shell electronic configuration. Many physical properties of rare gases *at low pressures* have been predicted by using *ab initio* or empirical two-body potentials such as the Lennard-Jones potentials, which consist of a short-range repulsive potential and a long-range attractive dispersion potential.[1, 2] At low temperatures, the rare gas atoms form van der Waals crystals of the fcc structure except helium, which crystallizes to the hcp structure. The crystal structure and the binding energy of rare gas solids have been determined very accurately by experiments. It has been found that two-body potentials can describe these properties very well. Although the two-body potentials underestimate the binding energy by a few percent, the inclusion of the three-body potentials as a small correction reduces the error to within one percent.[3, 4]

Recently, the development of Brillouin spectroscopy in conjunction with diamond-anvil cells (DAC's) [5] has opened the door for investigating the elastic properties of rare gas solids *at high pressures*, which may be important for earth and planetary sciences. The pressure dependence of the elastic stiffness coefficients has been experimentally determined up to 33 GPa by Grimsditch *et al.*[6] and up to 70 GPa by Shimizu *et al.*[7] The two groups used the *envelope method* to determine the elastic stiffness coefficients: the Brillouin frequency shifts are measured without identifying the crystal orientation. Then, the acoustic velocities calculated from the frequency shifts scatter because the acoustic velocity in crystals depends on the propagating direction. The maximum and minimum values of acoustic velocities at each pressure are determined and the *envelope curves* of the acoustic velocities are drawn. The elastic stiffness constants are determined by comparing the envelope curves with the solutions of the elastic equation. Shimizu *et al.*[7] also determined the elastic stiffness coefficients of solid argon from 1.6 GPa to 4 GPa by *in situ* Brillouin spectroscopy,[8] in which the crystal orientation is identified and more accurate results are obtainable. From the results of *in situ* Brillouin spectroscopy and the envelope method at high pressures, Shimizu *et al.*[7] found that solid argon becomes harder than iron [9] and that the deviation from the Cauchy relation becomes significant. The latter implies that the contribution of the non-central many-body force becomes more and more important at higher pressures, and it cannot be treated any longer as a small correction to the two-body potentials.

e-mail address: tiitaka@postman.riken.go.jp

Computational method

However, by now, calculations of elastic properties at high pressures have been limited to those with empirical two-body potentials [2, 6, 10] as at low pressures. In this study, therefore, we investigate the elastic stiffness coefficients of fcc solid argon at high pressures by using first-principles calculations with periodic boundary conditions [11–13] at zero temperature and under constant pressures, which can treat the effects of many-body potentials of crystals in a simple and direct way. The valence wave functions are expanded in a plane wave basis set truncated at a kinetic energy of 560 eV. The electron-ion interactions are described by the Vanderbilt-type ultrasoft pseudopotentials.[14] The effects of exchange-correlation interaction are treated within the generalized gradient approximation of Perdew *et al.* (GGA-PBE).[15] The model consists of an fcc unit cell containing four argon atoms. The Brillouin zones are sampled with $8 \times 8 \times 8$ Monkhorst-Pack k-points [16] by using time-reversal symmetry only. During the structural optimization, the enthalpy $H = E + PV$ is minimized by varying the length of the lattice vectors, while the angles between the lattice vectors and the atomic positions in the unit cell are fixed. In the geometrical optimization, the total stress tensor [17] is reduced to the order of 0.001 GPa by using the finite basis-set corrections.[18]

The elastic stiffness tensor c_{ijkl} relates the stress tensor σ_{ij} and the strain tensor ϵ_{kl} by Hooke's law,

$$\sigma_{ij} = c_{ijkl}\epsilon_{kl} \qquad (i, j, k, l = x, y, z). \tag{1}$$

Since the stress and strain tensors are symmetric, the most general elastic stiffness tensor has only 21 non-zero indepen-

dent components. For cubic crystals, they are reduced to three components, $c_{11} \equiv c_{xxxx}$, $c_{12} \equiv c_{xxyy}$, and $c_{44} \equiv c_{yzyz}$ (in the Voigt notation). These elastic stiffness coefficients can be determined by computing the stress generated by forcing a small strain to an optimized unit cell.[19, 20] The lattice vectors $\vec{a}_i'$ of the strained unit cell are determined from the lattice vectors $\vec{a}_i$ of the optimized unit cell by the relation $\vec{a}_i' = (I + \epsilon)\vec{a}_i$, where I is the unit matrix and ϵ is a strain tensor. Two strain tensors,

$$\epsilon^A = \begin{pmatrix} e & 0 & 0 \\ 0 & 0 & 0 \\ 0 & 0 & 0 \end{pmatrix}, \tag{2}$$

$$\epsilon^B = \begin{pmatrix} 0 & e/2 & 0 \\ e/2 & 0 & 0 \\ 0 & 0 & 0 \end{pmatrix}, \tag{3}$$

are used to determine the three elastic stiffness coefficients, c_{11}, c_{12}, and c_{44} from Eq. (1), namely, $\sigma^A_{xx} = c_{11}e$, $\sigma^A_{yy} = \sigma^A_{zz} = c_{12}e$, and $\sigma^B_{xy} = c_{44}e$ where σ^A and σ^B are the stresses resulting from straines ϵ^A and ϵ^B, respectively. The values of σ^A and σ^B are calculated with $e = 0$, 0.01, and 0.02 at each pressure, and fitted to a parabolic function of e to remove non-linear contributions. The convergence of the elastic stiffness coefficients with respect to the cut-off energy and the number of k-points was estimated to be of the order of 1 GPa by increasing the cutoff energy to 1120 eV and the Monkhorst-Pack k-points to $12 \times 12 \times 12$, respectively.

Results and discussion

Figure 1 shows the ρ–P equations of state. The agreement between the experiment and the GGA calculation indicates that the lattice constants of solid argon are mainly determined by the balance between the short-range repulsive force and the external pressure. The van der Waals force, which is not taken into account explicitly in the GGA calculation, is negligible in this pressure range.

Figure 2 shows the pressure dependence of the elastic stiffness coefficients, c_{11}, c_{12}, and c_{44}. The elastic stiffness coefficients increase linearly with increasing pressure. These elastic stiffness coefficients satisfy the generalized elastic stability criteria for cubic crystals under hydrostatic pressure,[21–23]

$$c_{11} + 2c_{12} > 0, \qquad c_{44} > 0, \qquad \text{and} \qquad c_{11} - c_{12} > 0. \tag{4}$$

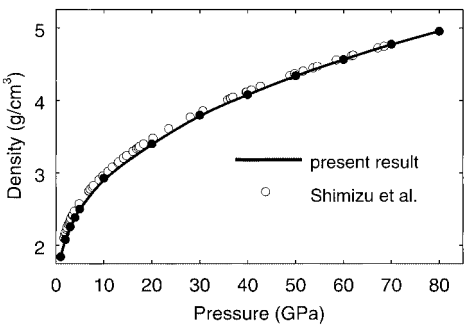

Fig. 1. $\rho - P$ equations of state for fcc solid argon. The solid curve with solid circles represents the present result. Open circles represent the experimental result obtained by Shimizu *et al.*[7] by means of Brillouin spectroscopy.

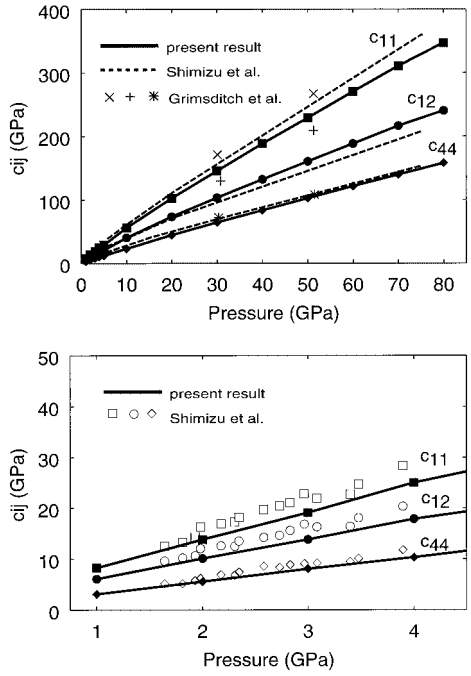

Fig. 2. Pressure dependence of the elastic stiffness coefficients, c_{11}, c_{12}, and c_{44} of fcc solid argon. Solid lines with closed symbols represent the present result. Dashed lines represent experimental result at 295 K obtained by the envelope method by Shimizu *et al.*[7] Cross symbols indicate the result of self-consistent phonon calculation based on pair potentials by Grimsditch *et al.*[6]

The agreement between the present and the experimental results for c_{11} and c_{12} does not appear to be very good between 10 GPa and 70 GPa. However, the agreement improves when the acoustic velocities are plotted as a function of the pressure as shown in Fig. 3.

Figure 3 shows the pressure dependence of the squares of the acoustic velocities, which are related to the elastic stiffness coefficients by

$$v^2_{LA,\max} = (c_{11} + 2c_{12} + 4c_{44})/(3\rho), \tag{5}$$

$$v^2_{LA,\min} = c_{11}/\rho, \tag{6}$$

$$v^2_{TA,\max} = c_{44}/\rho, \tag{7}$$

$$v^2_{TA,\min} = (c_{11} - c_{12})/(2\rho). \tag{8}$$

The agreement between the present result and the experimental one is better than that in Fig. 2, although theoretical $v_{TA,\min}$ above 10 GPa seems slightly smaller than the experimental data. The difference between the present result and the experimental result in Fig. 2 may depend on how the experimental envelope curves are drawn in Fig. 3.

Figure 4 shows the pressure dependence of the elastic anisotropy $A = 2c_{44}/(c_{11} - c_{12})$, which is the ratio of two shear moduli c_{44} and $(c_{11} - c_{12})/2$, and which becomes unity for isotropic elasticity. The anisotropy calculated between 1.6 and 4 GPa is approximately three, and agrees well with the experimental result. Above 4 GPa, the experimental anisotropy gradually decreases to two, while the present result is almost constant up to 80 GPa.

The deviation from the Cauchy relation $\delta = c_{12} - c_{44} - 2P$ is a measure of the contribution from the non-central many-

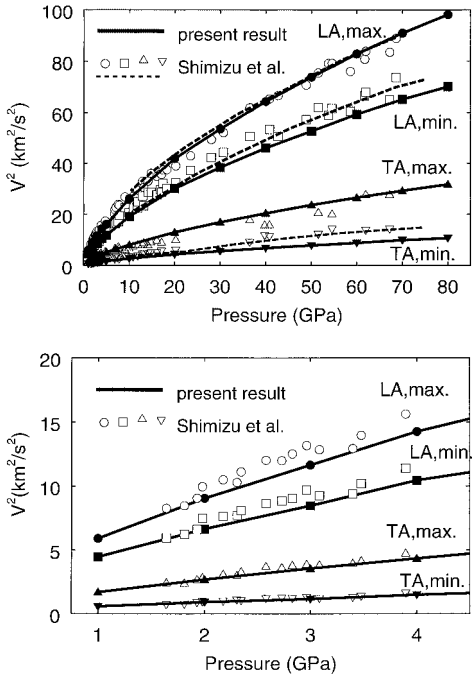

Fig. 3. Pressure dependence of the squares of acoustic velocities, $v^2_{LA,\max}$, $v^2_{LA,\min}$, $v^2_{TA,\max}$, and $v^2_{TA,\min}$, of fcc solid argon. Solid curves with closed symbols represent the present result. Open symbols represent the experimental data obtained by Shimizu *et al.*[7] The envelope method was used for the above 4 GPa and *in situ* Brillouin spectroscopy was used for the below 4 GPa. Dashed curves are the envelope curves for the experimental data.[7]

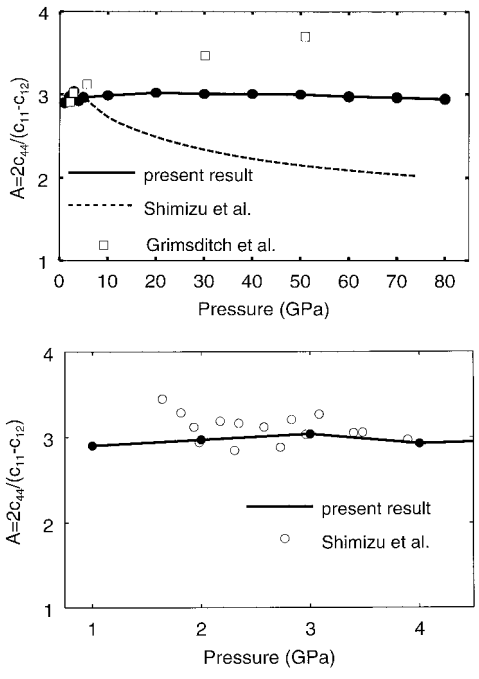

Fig. 4. Pressure dependence of the elastic anisotropy, $A = 2c_{44}/(c_{11} - c_{12})$, for fcc solid argon. Open squares represent the theoretical result by Grimsditch *et al.*[6] Other symbols and lines have the same meaning as in Fig. 3.

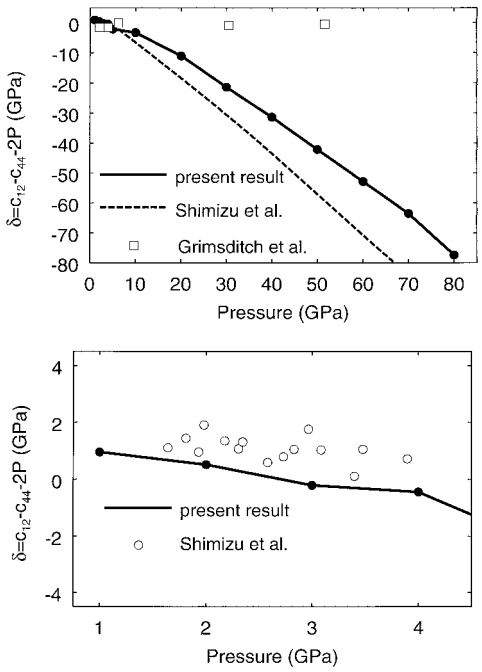

Fig. 5. Pressure dependence of the deviation from the Cauchy relation, $\delta = c_{12} - c_{44} - 2P$, for fcc solid argon. Symbols and lines have the same meanings as in Fig. 4.

body force since the Cauchy relation $c_{12} = c_{44} + 2P$ should be satisfied when interatomic potentials are purely central.[6, 24] Figure 5 shows the pressure dependence of δ. The deviation δ for the experimental result [7] becomes larger as the pressure increases, which indicates that the non-central many-body force becomes more and more important at high pressures. The δ of the present result agrees well with the experimental result, indicating that the first-principles calculation with the plane wave basis set and the pseudopotentials can correctly describe the many-body force. The δ for the theoretical result of Grimsditch *et al.* is almost zero for all pressures since their theory is based on pair potentials.

Summary

In summary, we computed the elastic properties of fcc solid argon at high pressure by using the first-principles calculation at zero temperature with the plane wave basis set, pseudopotentials and generalized gradient approximation for exchange-correlation interaction. We have shown that the standard density functional method with periodic boundary conditions at zero temperature and under constant pressures can be successfully applied for calculating the elastic properties of rare gas solids at high pressures in contrast to those at low pressures where dispersion forces are important. Although the effects of thermal and zero-point vibrations were not included in the present calculation, thermal effects are expected to be small at high pressures. The long-range van der Waals force is also not taken into account explicitly. However, the lattice constant and the elastic properties of solid argon at high pressures are mainly determined by the balance between the short-range repulsive force and the external pressure, and the van der Waals force is negligible.

The authors would like to thank G. J. Ackland and D. M. Bird

for valuable discussions and for providing the CASTEP code, and H. Shimizu and S. Sasaki for their encouragement and for providing their Brillouin spectroscopy data. The research presented here was undertaken within a joint collaboration between the Computational Science Division of RIKEN (The Institute of Physical and Chemical Research) and the United Kingdom Car-Parrinello (UKCP) consortium. The results presented here were computed by using supercomputers at RIKEN, ISSP, and NIG.

References

1) R. A. Aziz and M. J. Slaman: Mol. Phys. **58**, 679 (1986).
2) J. S. Tse, V. P. Shpakov, and V. R. Belosludov: Phys. Rev. B **58**, 2365 (1998).
3) V. F. Lotrich and K. Szalewicz: Phys. Rev. Lett. **79**, 1301 (1997).
4) K. Rosciszewski, B. Paulus, P. Fulde, and H. Stoll: Phys. Rev. B **62**, 5482 (2000).
5) H. Shimizu, E. M. Brody, H. K. Mao, and P. M. Bell: Phys. Rev. Lett. **47**, 128 (1981).
6) M. Grimsditch, P. Loubeyre, and A. Polian: Phys. Rev. B **33**, 7192 (1986).
7) H. Shimizu, H. Tashiro, T. Kume, and S. Sasaki: Phys. Rev. Lett. **86**, 4568 (2001).
8) H. Shimizu and S. Sasaki: Science **257**, 514 (1992).
9) V. V. Brazhkin and A. G. Lyapin: JETP Lett. **73**, 197 (2001).
10) F. Occelli, M. Krisch, P. Loubeyre, F. Sette, R. Le Toullec, C. Masciovecchio, and J.-P. Rueff: Phys. Rev. B. **63**, 224306 (2001).
11) I. Kwon, L. A. Collins, J. D. Kress, and N. Troullier: Phys. Rev. B **52**, 15165 (1995).
12) A. K. McMahan: Phys. Rev. B **33**, 5344 (1986).
13) M. C. Payne, M. P. Teter, D. C. Allan, T. A. Arias, and J. D. Joannopoulos: Rev. Mod. Phys. **64**, 1045 (1992); CASTEP 4.2 academic version, licensed under the UKCP-MSI Agreement, 1999.
14) D. Vanderbilt: Phys. Rev. B **41**, 7892 (1990).
15) J. P. Perdew, K. Burke, and M. Ernzerhof: Phys. Rev. Lett. **77**, 3865 (1996).
16) H. J. Monkhorst and J. D. Pack: Phys. Rev. B **13**, 5188 (1976).
17) O. H. Nielsen and R. M. Martin: Phys. Rev. Lett. **50**, 697 (1983).
18) G. P. Francis and M. C. Payne: J. Phys. Condens. Matter **2**, 4395 (1990).
19) R. M. Wentzcovitch, N. L. Ross, and G. D. Price: Phys. Earth Planet. Inter. **90**, 101 (1995).
20) B. B. Karki, L. Stixrude, S. J. Clark, M. C. Warren, G. J. Ackland, and J. Crain: Am. Mineral. **82**, 51 (1997).
21) J. Wang, S. Yip, S. R. Phillpot, and D. Wolf: Phys. Rev. Lett. **71**, 4182 (1993).
22) J. Wang, J. Li, S. Yip, S. Phillpot, and D. Wolf: Phys. Rev. B **52** 12627 (1995).
23) B. B. Karki, G. J. Ackland, and J. Crain: J. Phys. Condens. Matter **9**, 8579 (1997).
24) S. V. Sinogeikin and J. D. Bass: Phys. Rev. B **59**, R14141 (1999).